

Kernelized Classification in Deep Networks

Sadeep Jayasumana Srikumar Ramalingam Sanjiv Kumar
 Google Research, New York
 {sadeep, rsrikumar, sanjivk}@google.com

Abstract

In this paper, we propose a kernelized classification layer for deep networks. Although conventional deep networks introduce an abundance of nonlinearity for representation (feature) learning, they almost universally use a linear classifier on the learned feature vectors. We introduce a nonlinear classification layer by using the kernel trick on the softmax cross-entropy loss function during training and the scorer function during testing. Furthermore, we study the choice of kernel functions one could use with this framework and show that the optimal kernel function for a given problem can be learned automatically within the deep network itself using the usual backpropagation and gradient descent methods. To this end, we exploit a classic mathematical result on the positive definite kernels on the unit n -sphere embedded in the $(n + 1)$ -dimensional Euclidean space. We show the usefulness of the proposed nonlinear classification layer on several vision datasets and tasks.

1. Introduction

Deep learning, which is now a ubiquitous technique in machine learning, is built upon the premise that useful representations of the inputs can be automatically learned from data [4]. For example, in the image classification setting, a rich representation learning network consisting of building blocks such as convolution and max-pooling is first used to obtain a vector representation of the input image. This representation is commonly referred to as the *feature vector* of the input image.

The image is then classified into the correct class within the last layer of the network using a fully-connected layer operating on the feature vector [33, 17]. As will be demonstrated later, this last classification layer represents a linear classifier in the space of the learned feature vectors. Therefore, to perform well on the classification task, the classes have to be linearly separable in the space of feature vectors. While this is a standard assumption in many tasks, we wonder if using a nonlinear classifier on the learned feature vectors would give any additional benefits, especially when

the backbone feature extractor fails to learn fully linearly separable features.

Kernel methods is a different branch of machine learning that has been immensely successful in the pre-deep-learning era, particularly with the popularity of the Support Vector Machines (SVM) algorithm [9, 31]. Conventionally, kernel methods have been used for learning with hand-crafted feature vectors, such as the scale invariant feature transform (SIFT) [26], histogram-of-oriented-gradients (HOG) [12] and bag-of-visual-words [37] for image classification. The key idea in kernel methods is the following: instead of running a linear classifier on the feature vectors, they are first mapped to a higher-dimensional Reproducing Kernel Hilbert Space (RKHS) using a positive definite kernel function. For certain kernel functions, the RKHS can even be infinite dimensional. A linear classifier is then run on this high-dimensional RKHS. Since the dimensionality of the feature vectors is dramatically increased via this mapping, a linear classifier in the RKHS corresponds to a powerful nonlinear classifier in the original feature vector space. Such a classifier is capable of learning more complex patterns than a linear classifier directly operating on the feature vectors. Thanks to the kernel trick, we never have to explicitly calculate the high-dimensional vectors in the RKHS, which will be computationally expensive (or even impossible in the case of an infinite-dimensional space) to compute and store.

Although kernel methods yield excellent results in shallow machine learning in general, the choice of the kernel function is often problematic. There is a collection of well-known kernels such as the linear kernel, polynomial kernels, and the Gaussian RBF kernel [32, 31]. The Gaussian RBF kernel is a common choice; however, tuning its bandwidth parameter is non-trivial and different values for this parameter can give vastly different results.

In this work, we join the concepts of automatic representation learning and nonlinear, kernel-based classification. To this end, we formalize a nonlinear, kernelized classification layer for deep networks. To address the problem of choosing an appropriate kernel for the task, we take some results from classic mathematics literature on positive defi-

nite kernel functions and device a method that automatically learns the optimal kernel from data within the deep learning framework itself. As a result, the full network, which consists of a conventional representation learner and our kernelized classification layer, can be trained end-to-end using the usual backpropagation and gradient descent methods. We show the benefits of this framework in image classification, transfer learning, and distillation settings on a number of datasets.

2. Related Work

One of the earliest attempts to connect neural network based learning and kernel methods was the sigmoid kernel [34], which became popular in SVMs due to the early success of the neural networks. The design of this kernel function was inspired by the sigmoid activation function used in the early generations of neural networks. More recently, the authors of [7] proposed a family of kernel functions that mimic computations in large, multi-layer neural networks.

There have been a few methods that focus on extending the linear convolution in Convolutional Neural Networks to a nonlinear operation. Wang *et al.* [38] proposed a kernelized version of the convolution operation and demonstrated that it can learn more complicated features than the usual convolution operation. However, some kernels used in that work, such as the l^p -norm kernels, are not positive definite and hence do not represent a valid mapping to an RKHS. Convolutional kernel networks provides a kernel approximation scheme to interpret convolutions [27]. Other approaches include the use of Volterra series approximations to extend convolutions to a nonlinear operation by introducing quadratic terms [42].

In a related work [6], an RBF kernel layer is introduced to produce a feature space from pointcloud input. In contrast to our work, the RBF kernel layer is used on the input data and not in the classification layer.

Prior to the dominance of deep learning methods, picking the right kernel for a given problem has been studied extensively in works such as [19, 2, 20, 15]. In particular, Multiple Kernel Learning (MKL) approaches [15, 35] were popular in conjunction with SVM. Unfortunately, these methods scale poorly with the size of the training dataset. In this work, we automatically learn the kernel using the data within a deep network. This not only allows automatic representation learning, but also scales well for large training sets.

Kernels have also been considered for deep learning to reduce the memory footprint of CNNs. This was accomplished by achieving an end-to-end training of a Fastfood kernel layer [40], which uses approximations of kernel functions using Fastfood transforms [23].

Other related methods involving both kernels and deep

learning include scalable kernel methods [11], kernel pooling [10], deep SimNets [8], and deep kernel learning [39].

3. Nonlinear Softmax Loss

In this section, we formalize the kernelized classification in deep networks. Let us consider a multi-class classification problem with a training set $\{(x_i, y_i)\}_{i=1}^N$, where $x_i \in \mathcal{X}$ for each i , $y_i \in [L] = \{1, 2, \dots, L\}$ for each i , \mathcal{X} is a nonempty set, L is the number of labels, and N is the number of training examples. For example, each training data point (x_i, y_i) can be an image with its class label.

A deep neural network that solves this task has two components: a *representation learner* (also called the *feature learner*) and a *classifier*. In the case of image classification, the representation learner consists of modules such as convolution layers, max-pooling layers, and fully-connected layers. The classifier is the last fully-connected layer operating on the feature vectors, which is endowed with a loss function during training.

Let $r^{(\Theta)} : \mathcal{X} \rightarrow \mathbb{R}^d$ denote the representation learner, where d is the dimensionality of the learned feature vectors and Θ represents all the (learnable) parameters in this part of the network. The classifier is characterized by a function $g^{(\Omega)} : \mathbb{R}^d \rightarrow [L]$, where Ω denotes all the parameters in the last layer of the network. Usually, Ω consists of weight vectors $\mathbf{w}_1, \mathbf{w}_2, \dots, \mathbf{w}_L$ with each $\mathbf{w}_j \in \mathbb{R}^d$, and bias terms b_1, b_2, \dots, b_L with each $b_j \in \mathbb{R}$. The function $g^{(\Omega)}$ then takes the form:

$$g^{(\Omega)}(\mathbf{f}) = \operatorname{argmax}_j \mathbf{w}_j^T \mathbf{f}, \quad (1)$$

where $\mathbf{f} = r^{(\Theta)}(x) \in \mathbb{R}^d$ is the feature vector for input x . Note that we have dropped the additive bias term b_j to keep the notation uncluttered. There is no loss of generalization here since the bias term can be absorbed into \mathbf{w}_j by appending a constant element to \mathbf{f} . During inference, the deep network's class prediction \hat{y}^* for an input x^* is the composite of these two functions:

$$\hat{y}^* = \left(g^{(\Omega)} \circ r^{(\Theta)} \right) (x^*). \quad (2)$$

Although conceptually there are two components of the deep network, their parameters Θ and Ω are learned jointly during the training of the network. The de facto standard way of training a classification network is minimizing the *softmax loss* applied to the classification layer. The softmax loss is the combination of the softmax function and the cross-entropy loss. More specifically, for a single training example (x, y) with the feature vector $\mathbf{f} = r^{(\Theta)}(x)$, the softmax loss is calculated as,

$$l(y, \mathbf{f}) = -\log \left(\frac{\exp(\mathbf{w}_y^T \mathbf{f})}{\sum_{j=1}^L \exp(\mathbf{w}_j^T \mathbf{f})} \right). \quad (3)$$

Note that the classifier $g^{(\Omega)}$ trained in this manner is completely linear in \mathbb{R}^d , the space of the feature vectors \mathbf{f} s, as is evident from Eq. (2).

From the classic knowledge in kernel methods on hand-crafted features, we are aware that more powerful nonlinear classifiers on \mathbb{R}^d can be obtained using the kernel trick. The key idea here is to first embed the feature vectors \mathbf{f} s into a high-dimensional Reproducing Kernel Hilbert Space (RKHS) \mathcal{H} and perform classification in \mathcal{H} . Although the classification is linear in the high-dimensional Hilbert space \mathcal{H} , it is nonlinear in the original feature vector space \mathbb{R}^d . Let $\phi : \mathbb{R}^d \rightarrow \mathcal{H}$ represent this RKHS embedding. Performing classification in \mathcal{H} is then equivalent to training the neural network with the following modified version of the softmax loss:

$$l'(y, \mathbf{f}) = -\log \left(\frac{\exp(\langle \phi(\mathbf{w}_y), \phi(\mathbf{f}) \rangle_{\mathcal{H}})}{\sum_{j=1}^L \exp(\langle \phi(\mathbf{w}_j), \phi(\mathbf{f}) \rangle_{\mathcal{H}})} \right), \quad (4)$$

where $\langle \cdot, \cdot \rangle_{\mathcal{H}}$ denotes the inner product in the Hilbert space \mathcal{H} . The key difference between Eq. (3) and Eq. (4) is that the dot products between \mathbf{w}_j s and \mathbf{f} have been replaced with the inner products between $\phi(\mathbf{w}_j)$ s and $\phi(\mathbf{f})$. The more general notion of *inner product* is used instead of the *dot product* because the Hilbert space \mathcal{H} can be infinite dimensional.

For a network trained with this nonlinear version of the softmax function, the label prediction can be obtained using the following modified version of the predictor:

$$g'^{(\Omega)}(\mathbf{f}) = \operatorname{argmax}_j \langle \phi(\mathbf{w}_j), \phi(\mathbf{f}) \rangle_{\mathcal{H}}. \quad (5)$$

Note that the Hilbert space embeddings $\phi(\cdot)$ s can be very-high, even infinite, dimensional. Therefore, computing and storing them can be problematic. We can use the *kernel trick* in the classic machine learning literature [31, 32] to overcome this problem: explicit computation of $\phi(\cdot)$ s is avoided by directly evaluating the inner product between them using a kernel function $k : \mathbb{R}^d \times \mathbb{R}^d \rightarrow \mathbb{R}$. This idea is summarized by the equation:

$$\langle \phi(\mathbf{w}), \phi(\mathbf{f}) \rangle_{\mathcal{H}} = k(\mathbf{w}, \mathbf{f}). \quad (6)$$

For a kernel function to represent a valid RKHS, it must be positive definite [3, 5]. We discuss this notion next.

4. Kernels on the Unit Sphere

It was shown in the previous section that, given a kernel function on the feature vector space, we can obtain a nonlinear classifier in the last layer of a deep network by modifying the softmax loss function during training and the predictor during inference. However, only positive definite kernels allow this trick. There are various choices for

kernel functions in the classic machine learning literature. Some popular choices include the polynomial kernel, the Gaussian RBF kernel (squared exponential kernel), and the Laplacian kernel. However, in the classic kernel methods literature, there is no principled method for selecting the optimal kernel for a given problem. Furthermore, many of the kernels have hyperparameters that need to be manually tuned. The generally accepted solution to this problem in classic kernel methods is the MKL framework [15], where the optimal kernel is learned as a linear combination of some pre-defined kernels. Unfortunately, like SVM, MKL methods do not scale well with the train set size.

In this section, we present some theoretical results that will pave the way to define a neural network layer that can automatically learn the optimal kernel from data. By formulating kernel learning as a neural network layer, we inherit the desirable properties of deep learning, including scalability and automatic feature learning.

We start the discussion with the following definition of positive definite kernels [5].

Definition 4.1. Let \mathcal{U} be a nonempty set. A function $k : (\mathcal{U} \times \mathcal{U}) \rightarrow \mathbb{R}$ is called a **positive definite kernel** if $k(u, v) = k(v, u)$ for all $u, v \in \mathcal{U}$ and

$$\sum_{j=1}^N \sum_{i=1}^N c_i c_j k(u_i, u_j) \geq 0,$$

for all $N \in \mathbb{N}$, $\{u_1, \dots, u_N\} \subseteq \mathcal{U}$ and $\{c_1, \dots, c_N\} \subseteq \mathbb{R}$.

Properties of positive definite kernels have been studied extensively in mathematics literature [3, 29, 5]. The following proposition summarizes some important closure properties of this class of functions.

Proposition 4.2. The family of all positive definite kernels on a given nonempty set forms a convex cone that is closed under pointwise multiplication and pointwise convergence.

Proof. To intuitively understand this result, it is helpful to recall that the geometry of the family of all positive definite kernels on a given nonempty set is closely related to the geometry of the space of the $d \times d$ symmetric positive definite matrices, which forms a convex cone. The formal proof of this proposition can be found in Remark 1.11 and Theorem 1.12 of Chapter 3 of [5]. \square

To simplify the problem setting, we assume that both the feature vectors \mathbf{f} s and the weight vectors \mathbf{w}_j s are unit norm. Not only this simplifies the mathematics, but also it is a practice in use for stabilizing the training of neural networks [41]. Due to this assumption, we are interested in positive definite kernels on the unit sphere in \mathbb{R}^d . From now on, we use S^n , where $n = d - 1$, to denote this space.

We also restrict our discussion to radial kernels on S^n . Radial kernels, kernels that only depend on the distance between the two input points, have desirable property of translation invariance. Furthermore, all the commonly used kernels on S^n , such as the linear kernel, the polynomial kernel, the Gaussian RBF kernel, and the Laplacian kernel are radial kernels. The following theorem, origins of which can be traced back to [30], fully characterizes radial kernels on S^n .

Theorem 4.3. *A radial kernel $k : S^n \times S^n \rightarrow \mathbb{R}$ is positive definite for any n if and only if it admits a unique series representation of the form*

$$\begin{aligned} k(\mathbf{u}, \mathbf{v}) &= \sum_{m=0}^{\infty} \alpha_m \langle \mathbf{u}, \mathbf{v} \rangle^m \\ &+ \alpha_{-1} (\llbracket \langle \mathbf{u}, \mathbf{v} \rangle = 1 \rrbracket - \llbracket \langle \mathbf{u}, \mathbf{v} \rangle = -1 \rrbracket) \\ &+ \alpha_{-2} \llbracket \langle \mathbf{u}, \mathbf{v} \rangle \in \{-1, 1\} \rrbracket, \end{aligned} \quad (7)$$

where each $\alpha_m \geq 0$, $\sum_{m=-2}^{\infty} \alpha_m < \infty$, and $\llbracket \cdot \rrbracket$ depicts the Iverson bracket.

Proof. The kernel $k_1 : S^n \times S^n \rightarrow [-1, 1] : k_1(\mathbf{u}, \mathbf{v}) = \langle \mathbf{u}, \mathbf{v} \rangle$ is positive definite on S^n for any n since $\sum_j \sum_i c_i c_j \langle \mathbf{u}_i, \mathbf{u}_j \rangle = \|\sum_i c_i \mathbf{u}_i\|^2 \geq 0$. Therefore, from the closure properties in Proposition 4.2, the kernel $k_m : (\mathbf{u}, \mathbf{v}) \mapsto \langle \mathbf{u}, \mathbf{v} \rangle^m$ is also positive definite on S^n for any $m \in \mathbb{N}$. Furthermore, k_m is positive definite for $m = 0$ since $\sum_j \sum_i c_i c_j \langle \mathbf{u}_i, \mathbf{u}_j \rangle^0 = \|\sum_i c_i \mathbf{u}_i\|^2 \geq 0$.

Let us now consider the following two sequences of kernels:

$$\begin{aligned} s_{\text{odd}} &= k_1, k_3, \dots, k_{2m+1}, \dots \text{ and} \\ s_{\text{even}} &= k_2, k_4, \dots, k_{2m}, \dots \end{aligned}$$

Since $-1 \leq \langle \mathbf{u}, \mathbf{v} \rangle \leq 1$, it is clear that s_{odd} and s_{even} converge pointwise to the following kernels, respectively.

$$\begin{aligned} k_{\text{odd}}(\mathbf{u}, \mathbf{v}) &= \llbracket \langle \mathbf{u}, \mathbf{v} \rangle = 1 \rrbracket - \llbracket \langle \mathbf{u}, \mathbf{v} \rangle = -1 \rrbracket, \\ k_{\text{even}}(\mathbf{u}, \mathbf{v}) &= \llbracket \langle \mathbf{u}, \mathbf{v} \rangle \in \{-1, 1\} \rrbracket. \end{aligned}$$

From the last closure property of Proposition 4.2, both k_{odd} and k_{even} are positive definite on S^n . Invoking Proposition 4.2 again, we conclude that any finite conic combination of the kernels $k_{\text{even}}, k_{\text{odd}}, k_0, k_1, \dots$ is positive definite on S^n for any n . This completes the forward direction of the proof.

For the proof of the converse, we refer the reader to Theorem 3.6 in Chapter 5 of [5]. \square

Equipped with a complete characterization of the positive definite radial kernels on S^n , we now discuss how we can combine this result with the nonlinear softmax formulation derived in Section 3 to automatically learn the best kernel classifier within a deep network.

5. The Kernelized Classification Layer

We are now ready to describe our full framework for nonlinear classification in the feature space. We introduce a kernelized classification layer that acts as a drop-in replacement for the usual softmax classification layer in a deep network. This new layer classifies feature vectors in a high-dimensional RKHS while automatically choosing the optimal positive definite kernel that enables the mapping into the RKHS. As a result, we do not have to hand-pick a kernel or its hyperparameters.

5.1. Mechanics of the Layer

The new classification layer is parameterized by the usual weight vectors: $\mathbf{w}_1, \mathbf{w}_2, \dots, \mathbf{w}_L$, and some additional learnable coefficients: $\alpha_{-2}, \alpha_{-1}, \dots, \alpha_M$, where $M \in \mathbb{N}$ and each $\alpha_m \geq 0$. During training, this classifier maps feature vectors \mathbf{f} s to a high-dimensional RKHS \mathcal{H}_{opt} , which optimally separates feature vectors belonging to different classes, and learns a linear classifier in \mathcal{H}_{opt} . During inference, the classifier maps feature vectors of previously unseen input to the RKHS it learned during training and performs classification in that space. This is achieved by using the nonlinear softmax loss defined in Eq (4) during training and the nonlinear predictor defined in Eq (5) during testing, with the inner product in \mathcal{H} given by:

$$\langle \phi(\mathbf{w}), \phi(\mathbf{f}) \rangle_{\mathcal{H}} = \langle \phi(\mathbf{w}), \phi(\mathbf{f}) \rangle_{\mathcal{H}_{\text{opt}}} = k_{\text{opt}}(\mathbf{w}, \mathbf{f}), \quad (8)$$

where $k_{\text{opt}}(\cdot, \cdot)$ is the reproducing kernel of \mathcal{H}_{opt} . The optimal RKHS \mathcal{H}_{opt} for a given classification problem is learned by finding the optimal kernel k_{opt} during training as discussed in the following.

Theorem 4.3 states that any positive definite radial kernel on S^n admits the series representation shown in Eq. (7). Therefore, the optimal kernel k_{opt} must also have such a series representation. We approximate this series with a finite summation by cutting off the terms beyond the order M . More specifically, we use:

$$\begin{aligned} k_{\text{opt}}(\mathbf{w}, \mathbf{f}) &\approx \sum_{m=0}^M \alpha_m k_m(\mathbf{w}, \mathbf{f}) + \alpha_{-1} k_{\text{odd}}(\mathbf{w}, \mathbf{f}) \\ &\quad + \alpha_{-2} k_{\text{even}}(\mathbf{w}, \mathbf{f}), \end{aligned} \quad (9)$$

where, $k_{\text{even}}, k_{\text{odd}}, k_0, k_1, \dots, k_M$ have meanings defined Section 4 and $\alpha_{-2}, \alpha_{-1}, \dots, \alpha_M \geq 0$. Using Proposition 4.2 and the discussion in the proof of Theorem 4.3, one can easily verify that this approximation does not violate the positive definiteness of k_{opt} .

With this, k_{opt} is learned automatically from data by making the coefficients $\alpha_{-2}, \alpha_{-1}, \dots, \alpha_M$ s learnable parameters of the classification layer. Let $\alpha = [\alpha_{-2}, \alpha_{-1}, \dots, \alpha_M]^T$. The gradient of the loss function

with respect to α can be easily calculated via the back-propagation algorithm using the equations (4), (8), and (9). Therefore, it can be optimized along with $\mathbf{w}_1, \mathbf{w}_2, \dots, \mathbf{w}_L$ during the gradient descent based optimization of the network. This procedure is equivalent to automatically finding the RKHS that optimally separates the feature vectors belonging to different classes.

The constraint $\alpha_{-2}, \alpha_{-1}, \dots, \alpha_M \geq 0$ in Eq. (9) can be imposed with the commonly used ReLU operation. We discuss this in more detail in Section 5.2. As for the number of kernels M in the approximation, as long as it is sufficiently large, the exact value of M is not critical. This is because, as discussed in the proof of Theorem 4.3, the higher order terms that are truncated approach either k_{odd} or k_{even} , both of which are already included in the finite summation. On the flip side, if the terms beyond some order $M' < M$ are not important, the network can automatically learn to make the corresponding α coefficients vanish. In practice, we observed that 10 kernels work well enough and stick to this number in all our experiments.

Importantly, the kernelized classification layer described above can pass on the gradients of the loss to its inputs: the feature vectors \mathbf{f} s. Therefore, our kernelized classification layer is fully compatible with end-to-end training and can act as a drop-in replacement for an existing softmax classification layer.

5.2. Regularization of the Coefficients

The constraint $\alpha_{-2}, \alpha_{-1}, \dots, \alpha_M \geq 0$ is important in order to preserve the positive definiteness of k_{opt} . As noted above, this can be straightforwardly imposed by using $\alpha = \text{ReLU}(\alpha')$, where α' is the learnable parameter vector. However, ReLU has no upper-bound and allowing the scale of α to grow unboundedly causes the following issue in optimization: Assume we have an instantiation α_0 of the vector α . By replacing α_0 with $\lambda\alpha_0$, where $\lambda > 1$, we scale all the inner product terms in Eq. (4) and Eq. (5) by the same λ . As a result, we improve the loss of the already correctly classified training examples, but without making any effective change to the predictor. This is analogous to decreasing the temperature [18] of the softmax loss. Therefore, under this setting, once the majority of the training examples are correctly classified, the neural network can easily improve the loss just by increasing the norm of α , which is not useful. We therefore advocate an l^2 -regularization (weight decay) term on α when ReLU activation is used.

Alternatively, one could also use $\alpha = \text{sigmoid}(\alpha')$ or $\alpha = \text{softmax}(\alpha')$, both of which not only guarantee $\alpha_{-2}, \alpha_{-1}, \dots, \alpha_M \geq 0$, but also produce bounded α . Therefore, no regularization on α is needed for these options. The softmax activation here should not be confused with the softmax loss discussed in Section 3. The usage of the softmax activation in this context is similar to that in

the self-attention literature [36], where it is used to normalize the coefficients of a linear combination. Note also that both ReLU and sigmoid are elementwise operations on α' , while softmax is a vector operation.

5.3. Usage in the Distillation Setting

We expect the kernelized classification to be particularly useful in settings where the capacity of the feature learning or backbone network is capacity limited. This is because a capacity-limited network might not be able to learn fully linearly separable features and therefore a nonlinear classifier can be useful to augment its capabilities.

Another common method used to improve classification with capacity-limited networks is knowledge distillation [18], where the logit or probability outputs of a larger *teacher* network is used to train a smaller *student* network. While training the student network, the loss function (partially) consists of the cross-entropy loss with the teacher network's output. More specifically, using the same notation as in Section 3, assume that for a training example (x, y) , the teacher produces logits $\mathbf{h} = [h_1, h_2, \dots, h_L]^T$. Then, for the student network with the feature vector $\mathbf{f} = r^{(\Theta)}(x)$ and a usual classification layer parameterized by the weight vectors $\mathbf{w}_1, \mathbf{w}_2, \dots, \mathbf{w}_L$, the cross-entropy loss is given by:

$$l_{\text{st}}(\mathbf{h}, \mathbf{f}) = - \sum_{j'=1}^L \tilde{h}_{j'} \log \left(\frac{\exp(\mathbf{w}_{h'}^T \mathbf{f} / T)}{\sum_{j=1}^L \exp(\mathbf{w}_j^T \mathbf{f} / T)} \right), \quad (10)$$

where $\tilde{h}_{j'} = \exp(h_{j'}/T) / \sum_{j=1}^L \exp(h_j/T)$ and T is the temperature hyperparameter.

In distillation, the student network tries to imitate a teacher network, which is capable of producing more powerful feature vectors than the student. Intuitively, therefore, the student could benefit from using a powerful nonlinear classifier on the weak feature vectors it produces. With this mind, we explore the use of kernelized classification layer in the student network. The cross-entropy loss with the teacher scores in this case is:

$$l'_{\text{st}}(\mathbf{h}, \mathbf{f}) = - \sum_{j'=1}^L \tilde{h}_{j'} \log \left(\frac{\exp(\langle \phi(\mathbf{w}_{j'}), \phi(\mathbf{f}) \rangle_{\mathcal{H}} / T)}{\sum_{j=1}^L \exp(\langle \phi(\mathbf{w}_j), \phi(\mathbf{f}) \rangle_{\mathcal{H}} / T)} \right), \quad (11)$$

where all the terms have meanings defined earlier.

6. Experiments

In this section, we present experimental evaluations of our method. Note that our focus is to validate the theory presented in the previous sections and demonstrate its efficacy, not to claim state-of-the-art results on the already well explored image classification datasets.

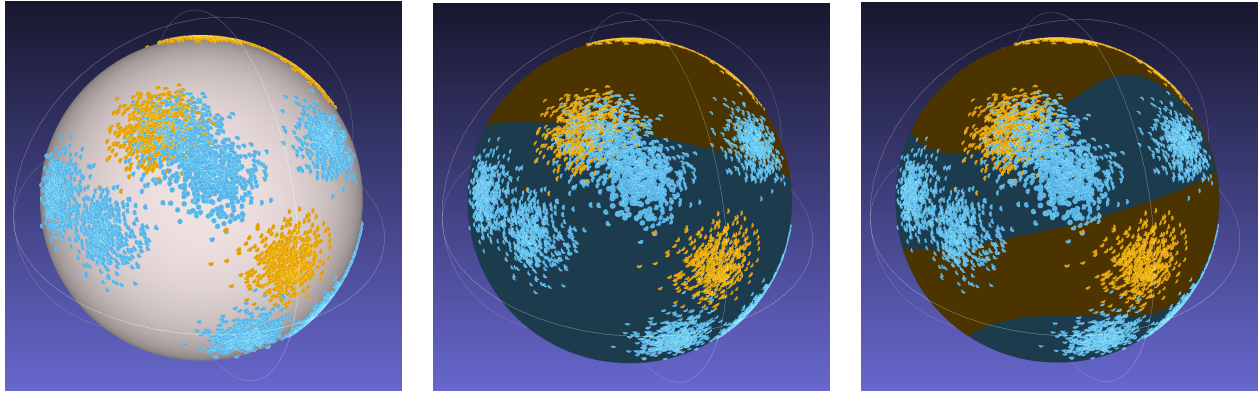


Figure 1. **Classification of a binary synthetic dataset on S^2 .** In the second and third images, binary regions identified by the respective classifiers are shown in blue and orange colors. Training data has been overlaid in all three images. Note that the softmax classifier (middle) can only separate cap-like regions on the sphere, whereas our kernelized classifier (right) can do more complex nonlinear classification thanks to the higher dimensional RKHS embedding of the sphere. Best viewed in color.

For each experiment, our baseline method used the standard softmax-based classifier. To evaluate our method, we replaced this classification layer with our proposed kernelized classification layer. In all experiments we use 10 kernels, meaning that the kernelized classification layer uses only 10 additional learnable parameters. As discussed in Section 5.2, we also used ReLU activation and a weight decay of 0.0001 on this 10-dimensional parameter vector. This is the same amount of weight decay used in the other parts of the network. This vector was initialized to have all ones in all our experiments.

To keep the number of learnable parameters comparable, we keep the additive bias term in the baseline classifier and omit them in the kernelized classifier. This bias terms introduces a number of learnable parameters equal to the number of classes used. Therefore, in most cases, the baseline model actually uses more learnable parameters than the kernelized classifier.

We also removed the ReLU activation on the feature vectors to utilize the full surface of S^n . We did the same to the baseline model as well to enable a fair comparison. For the baseline model, removal of the ReLU activation or the normalization of the feature vectors did not make a significant difference in the accuracy (see Section 6.5 for more details).

Throughout the experiments, we SGD with momentum 0.9, linear learning rate warmup [14], cosine learning rate decay [25], and decide the base learning by cross validation. When a better learning rate schedule is available for the baseline (e.g. CIFAR schedule in [17]), we experimented with both that and our schedule and report the best accuracy of the two. The maximum number of epochs was 450 in all cases. Mini-batch size was 128 for the synthetic and CIFAR datasets and 64 other datasets with larger images. We used the CIFAR data augmentation method in [17] for

Method	Accuracy
Softmax classifier (baseline)	85.51
Kernelized classifier (ours)	94.20
Bayes optimal classifier	95.06

Table 1. **Results on the synthetic dataset.** Note that the accuracy of the kernelized classifier is close to that of the ideal Bayes optimal classifier (theoretical maximum).

CIFAR-10 and CIFAR-100 datasets, and the Imagenet data augmentation in the same paper for other image datasets.

6.1. Synthetic Data

We use our first experiment to evaluate the proposed kernelized classification layer as an isolated unit by demonstrating its capabilities to learn nonlinear patterns on S^n . To this end, inspired by the blue-orange dataset used in Chapter 2 of [16], we generated a two-class dataset on S^2 with a mixture of Gaussian clusters for each class. More specifically, we first generated 10 cluster centers for each class by sampling from an isotropic Gaussian distribution with covariance $0.5 I_3$ and mean $[1, 0, 0]^T$ for the first class and $[0, 1, 0]^T$ for the second class. We then generated 5,000 observations for each class using the following method: for each observation, we uniform-randomly picked a cluster center and then generated a sample from an isotropic Gaussian distribution centered at that cluster center with covariance $0.02 I_3$. All the observations were projected on to S^2 by l^2 normalizing them.

We then considered these observations as feature vectors and trained a usual softmax-based classification layer (baseline) and our kernelized classification layer on them for comparison. Results on a test set generated in the same manner are shown in Table 1. We also report the theo-

retical maximum accuracy, the accuracy of the Bayes optimal classifier [16], which we can calculate for this synthetic dataset since we know the data generating model. It is noteworthy that the accuracy of our kernelized classification layer significantly outperforms the baseline and gets close to the Bayes optimal performance. This can be attributed to the layer’s capabilities to learning nonlinear patterns on the sphere by embedding the data into a much higher dimensional RKHS.

We visualize our training data, the baseline classifier’s output and the kernelized classifier’s output in Figure 1. Note that the usual softmax classifier can only separate cap-like regions on S^2 , this is a result of its being a linear classifier with respect to the feature vectors. Our kernelized classifier, on the other hand, can do a more complex nonlinear separation of the data.

6.2. Image Classification

We now report results on CIFAR-10 and CIFAR-100 real world image benchmarks [22]. For each dataset, we experimented with several CIFAR ResNet architectures [17]. Results are summarized in Table 2. In all cases our method significantly outperforms the baseline.

Representation Learner	CIFAR-10		CIFAR-100	
	Baseline	Ours	Baseline	Ours
ResNet-8	83.73	86.93	53.82	58.27
ResNet-14	89.87	91.48	63.85	66.67
ResNet-20	91.14	92.88	65.99	69.33
ResNet-32	92.22	93.70	68.96	71.30
ResNet-44	92.10	94.05	70.16	73.20
ResNet-56	93.01	94.15	71.23	74.10

Table 2. **Results on CIFAR-10 and CIFAR-100 datasets.** Accuracy of the proposed kernelized classifier is higher than the that of the baseline in all cases.

6.3. Transfer Learning

In the next set of experiments we evaluate our method in a transfer learning setting. To this end, we take a ResNet-50 network pre-trained on the Imagenet ILSVRC 2012 classification dataset [13] and fine tune it Oxford-IIIT Pets [28] and Stanford Cars [21] datasets. For each dataset, we use the train/test splits provided by the standard Tensorflow Datasets implementation [1]. Results are summarized in Table 3. On both datasets, kernelized classification layer results in significant gains. This is intuitive to understand since the feature vectors learned from the source task might not linearly separate the new classes in the target task. We can therefore benefit from a nonlinear classifier in this setting.

Method	Accuracy	
	Baseline	Ours
Oxford-IIIT Pets	92.06	93.56
Stanford Cars	90.78	92.60

Table 3. **Results on the transfer learning datasets.** Accuracy of the proposed kernelized classifier is higher than that of the baseline on both datasets.

6.4. Knowledge Distillation

We now demonstrate the capabilities of our method in the distillation setting discussed in Section 5.3. We used the CIFAR-10 and CIFAR-100 datasets, the baseline CIFAR ResNet-56 models from Table 2 as the teacher models, and the LeNet-5 network [24] as the student model. We use only the cross-entropy loss with the teacher scores with the temperature parameter T set to 20 in all cases. Results are shown in Table 4. Once again, significant gains are observed with the kernelized classification layer. This can be attributed to its capabilities to approximate complex teacher probabilities even with weak features.

Method	Accuracy	
	Baseline	Ours
CIFAR-10	76.06	79.85
CIFAR-100	44.38	46.48

Table 4. **Results in the distillation setting.** Accuracy of the proposed nonlinear classifier is higher than that of the baseline in all cases.

6.5. Ablation Studies

We conclude our experimental evaluation with a number of ablation studies and other analyses. For all the studies below, we used the CIFAR-100 dataset and the ResNet-56 backbone network.

6.5.1 Normalization

As discussed earlier, we use l^2 normalization on both the features and the weight vectors in the classification layer. One can wonder what the effect of a similar normalization would be on the baseline model. To answer this question, we experimented with a setup where we used normalized embeddings and normalized weight vectors in the usual softmax loss (Eq. (3)). Out of the box, this had significantly lower performance than softmax loss with unnormalized features/weights. This is because when both features and weights are normalized, we have the restriction $-1 \leq \mathbf{w}_j^T \mathbf{f} \leq 1$ in Eq. (3) which cripples the usual softmax loss function. This can, however, be circumvented by using an appropriate temperature parameter [18]. In this setting, the performance of the softmax classifier stays largely

stable as long as the temperature parameter is small enough. This is consistent with what authors of [41] have observed. We summarize our results in Table 5, where we used a temperature of 0.05. Note that making the temperature a learnable parameter has the same optimization issue outlined in Section 5.2.

In all the experiments in the previous sections, we use normalized features for the baseline (row 3 in Table 5), which we believe to provide a level playing field without limiting the capabilities of the softmax classifier.

Method	Accuracy
Softmax classifier with:	
no normalization	71.16
features normalized	71.23
features & weights normalized	60.34
features & weights normalized with temp.	70.43
Kernelized classifier (ours)	74.10

Table 5. **Effect of the normalization of features and weights.** Normalizing both features and weights cripples the softmax classifier, but it can be circumvented by using an appropriate temperature (0.05 in this case).

6.5.2 Feature rectification

Another thing we do differently to the usual image classification networks such as ResNet [17], is removing the ReLU activation from the feature vectors. We do this in order to utilize the full surface of S^n without restricting ourselves to only the nonnegative orthant. As is evident from Table 6, removing ReLU has only a marginal effect on the baseline. It is however an important factor for our method.

In all our experiments in the previous sections we used feature vectors without the ReLU activation.

Method	Accuracy
Softmax classifier with:	
rectified features	70.96
unrectified features	71.23
Kernelized classifier with:	
rectified features	71.61
unrectified features	74.10

Table 6. **Effect of rectification of the feature vectors.** Using unrectified feature vectors is important for the kernelized classifier.

6.5.3 Activation on the kernel coefficients

As discussed in Section 5.2, we have several choices to impose the constraint that kernel coefficients α_m s are non-negative. Using the notation from that section, we experimented with ReLU, sigmoid, and softmax activations on α' and summarized the results in Table 7.

Due to the reasons discussed in Section 5.2, we used a weight decay of 0.0001 on the coefficient vector whenever ReLU activation is used. Although sigmoid and softmax activations eliminate the need for weight decay, they put a hard constraint on $|k_{\text{opt}}(.,.)|$ and therefore $|\langle \phi(\mathbf{w}), \phi(\mathbf{f}) \rangle_{\mathcal{H}}|$. To overcome this limitation, it is helpful to use a temperature hyperparameter in Eq. (4), where each inner product is multiplied by $1/T$ before taking the exponential. We used a temperature of 0.1 and 0.005, with sigmoid and softmax, respectively. Although sigmoid gives the best performance in Table 7, we occasionally observed optimization issues with it, which might be due to the vanishing gradient issue associated with this activation function. We therefore stick to ReLU in all other experiments. We however note that, in most cases, competitive results can be obtained with softmax as well, when used with a temperature of 0.005.

It is also interesting to note that using no activation function on α' causes frequent divergence in training. This is consistent with the theory: The summation in Eq. (9) is not guaranteed to be positive definite when α_m s are allowed to be negative (see Proposition 4.2). Therefore, the theory of kernelized classification is not valid in this case.

Activation function	Accuracy
sigmoid	74.96
softmax	73.69
ReLU	74.10
None (linear)	unstable

Table 7. **Different activation functions on the coefficient vector.** Note that the kernelized classifier is unstable when no activation function is used, this agrees with the theoretical analysis.

6.5.4 Learning of the kernel coefficients

To investigate what benefits automatic learning of the kernel gives us, we performed an experiment where we kept the coefficient vector α fixed at the initial value, all ones, throughout the training. Results are shown in Table 8.

Method	Accuracy
Coefficients fixed	73.16
Coefficients trained	74.10

Table 8. **Effect of training the kernel coefficient vector.** End-to-end training of the coefficient vector with the rest of the network gives the best results.

7. Conclusion

We presented a kernelized classification layer for deep neural networks. This classification layer classifies feature vectors in a high dimensional RKHS while automat-

ically learning the optimal kernel that enables this high-dimensional embedding. We showed substantial accuracy improvements with this layer in the image classification, transfer learning, and distillation settings. These accuracy improvements are due to the kernelized classification layer’s capability in finding nonlinear patterns in the feature vectors.

In the future, we plan to extend this idea to other loss functions such as regression losses and other tasks such as object detection and semantic image segmentation.

References

- [1] TensorFlow Datasets: a collection of ready-to-use datasets. [Online; accessed Nov-10-2020]. [7](#)
- [2] Shawkat Ali and Kate A. Smith-Miles. A meta-learning approach to automatic kernel selection for support vector machines. *Neurocomputing*, 2006. Neural Networks. [2](#)
- [3] Nachman Aronszajn. Theory of Reproducing Kernels. *Transactions of the American Mathematical Society*, 1950. [3](#)
- [4] Y. Bengio, A. Courville, and P. Vincent. Representation learning: A review and new perspectives. *IEEE Transactions on Pattern Analysis and Machine Intelligence*, 35(8):1798–1828, 2013. [1](#)
- [5] C. Berg, J. P. R. Christensen, and P. Ressel. *Harmonic Analysis on Semigroups*. Springer, 1984. [3](#), [4](#)
- [6] Weikai Chen, Xiaoguang Han, Guanbin Li, Chao Chen, Jun Xing, Yajie Zhao, and Hao Li. Deep rbfnet: Point cloud feature learning using radial basis functions, 2019. [2](#)
- [7] Youngmin Cho and Lawrence K. Saul. Kernel methods for deep learning. In Y. Bengio, D. Schuurmans, J. D. Lafferty, C. K. I. Williams, and A. Culotta, editors, *Advances in Neural Information Processing Systems 22*, pages 342–350. Curran Associates, Inc., 2009. [2](#)
- [8] Nadav Cohen, Or Sharir, and Amnon Shashua. Deep simnets. *CoRR*, abs/1506.03059, 2015. [2](#)
- [9] C. Cortes and V. Vapnik. Support Vector Networks. *Machine Learning*, 1995. [1](#)
- [10] Y. Cui, F. Zhou, J. Wang, X. Liu, Y. Lin, and S. Belongie. Kernel pooling for convolutional neural networks. In *2017 IEEE Conference on Computer Vision and Pattern Recognition (CVPR)*, 2017. [2](#)
- [11] Bo Dai, Bo Xie, Niao He, Yingyu Liang, Anant Raj, Maria-Florina Balcan, and Le Song. Scalable kernel methods via doubly stochastic gradients, 2015. [2](#)
- [12] Navneet Dalal and Bill Triggs. Histograms of Oriented Gradients for Human Detection. In *CVPR*, 2005. [1](#)
- [13] J. Deng, W. Dong, R. Socher, L.-J. Li, K. Li, and L. Fei-Fei. ImageNet: A Large-Scale Hierarchical Image Database. In *CVPR09*, 2009. [7](#)
- [14] Priya Goyal, Piotr Dollár, Ross B. Girshick, P. Noordhuis, L. Wesolowski, Aapo Kyrola, Andrew Tulloch, Y. Jia, and Kaiming He. Accurate, Large Minibatch SGD: Training ImageNet in 1 Hour. *ArXiv*, abs/1706.02677, 2017. [6](#)
- [15] Mehmet Gönen, Ethem Alpaydin, and Francis Bach. Multiple kernel learning algorithms. *JMLR*, 2011. [2](#), [3](#)
- [16] Trevor Hastie, Robert Tibshirani, and Jerome Friedman. *The Elements of Statistical Learning*. Springer Series in Statistics. Springer New York Inc., New York, NY, USA, 2001. [6](#), [7](#)
- [17] K. He, X. Zhang, S. Ren, and J. Sun. Deep residual learning for image recognition. In *2016 IEEE Conference on Computer Vision and Pattern Recognition (CVPR)*, pages 770–778, 2016. [1](#), [6](#), [7](#), [8](#)
- [18] Geoffrey Hinton, Oriol Vinyals, and Jeffrey Dean. Distilling the Knowledge in a Neural Network. In *NIPS Deep Learning and Representation Learning Workshop*, 2015. [5](#), [7](#)
- [19] Tom Howley and Michael G. Madden. The genetic kernel support vector machine: Description and evaluation. *Artif. Intell. Rev.*, 2005. [2](#)
- [20] Sadeep Jayasumana, Richard Hartley, Mathieu Salzmann, Hongdong Li, and Mehrtash Harandi. Optimizing Over Radial Kernels on Compact Manifolds. In *Conference on Computer Vision and Pattern Recognition (CVPR)*, 2014. [2](#)
- [21] Jonathan Krause, Michael Stark, Jia Deng, and Li Fei-Fei. 3d object representations for fine-grained categorization. In *4th International IEEE Workshop on 3D Representation and Recognition (3DRR-13)*, Sydney, Australia, 2013. [7](#)
- [22] Alex Krizhevsky. Learning multiple layers of features from tiny images. Technical report, 2009. [7](#)
- [23] Quoc Le, Tamás Sarlós, and Alex Smola. Fastfood: Approximating kernel expansions in loglinear time. In *ICML*, 2013. [2](#)
- [24] Yann Lecun, Léon Bottou, Yoshua Bengio, and Patrick Haffner. Gradient-based learning applied to document recognition. In *Proceedings of the IEEE*, pages 2278–2324, 1998. [7](#)
- [25] I. Loshchilov and F. Hutter. Sgdr: Stochastic gradient descent with warm restarts. In *International Conference on Learning Representations (ICLR) 2017 Conference Track*, Apr. 2017. [6](#)
- [26] David G Lowe. Distinctive image features from scale-invariant keypoints. *International journal of computer vision*, 60(2):91–110, 2004. [1](#)
- [27] Julien Mairal, Piotr Koniusz, Zaïd Harchaoui, and Cordelia Schmid. Convolutional kernel networks. *CoRR*, abs/1406.3332, 2014. [2](#)
- [28] O. M. Parkhi, A. Vedaldi, A. Zisserman, and C. V. Jawahar. Cats and dogs. In *2012 IEEE Conference on Computer Vision and Pattern Recognition*, 2012. [7](#)
- [29] I. J. Schoenberg. Metric Spaces and Positive Definite Functions. *Transactions of the American Mathematical Society*, 1938. [3](#)
- [30] I. J. Schoenberg. Positive Definite Functions on Spheres. *Duke Mathematical Journal*, 1942. [4](#)
- [31] Bernhard Schölkopf and Alexander J. Smola. *Learning with Kernels: Support Vector Machines, Regularization, Optimization, and Beyond*. MIT Press, 2002. [1](#), [3](#)
- [32] John Shawe-Taylor and Nello Cristianini. *Kernel Methods for Pattern Analysis*. Cambridge University Press, 2004. [1](#), [3](#)
- [33] K. Simonyan and A. Zisserman. Very Deep Convolutional Networks for Large-Scale Image Recognition. In *ICLR*, 2015. [1](#)

- [34] Vladimir N. Vapnik. *The Nature of Statistical Learning Theory*. Springer-Verlag, Berlin, Heidelberg, 1995. [2](#)
- [35] Manik Varma and D. Ray. Learning the discriminative power-invariance trade-off. In *IN ICCV*, 2007. [2](#)
- [36] Ashish Vaswani, Noam Shazeer, Niki Parmar, Jakob Uszkoreit, Llion Jones, Aidan N Gomez, Łukasz Kaiser, and Illia Polosukhin. Attention is All you Need. In *Advances in Neural Information Processing Systems*, 2017. [5](#)
- [37] A. Vedaldi, V. Gulshan, M. Varma, and A. Zisserman. Multiple kernels for object detection. In *2009 IEEE 12th International Conference on Computer Vision*, pages 606–613, 2009. [1](#)
- [38] Chen Wang, Jianfei Yang, Lihua Xie, and Junsong Yuan. Kervolutional neural networks. In *Proceedings of the IEEE Conference on Computer Vision and Pattern Recognition*, pages 31–40, 2019. [2](#)
- [39] Andrew Gordon Wilson, Zhiting Hu, Ruslan Salakhutdinov, and Eric P. Xing. Deep kernel learning. *CoRR*, abs/1511.02222, 2015. [2](#)
- [40] Z. Yang, M. Moczulski, M. Denil, N. De Freitas, L. Song, and Z. Wang. Deep fried convnets. In *2015 IEEE International Conference on Computer Vision (ICCV)*, 2015. [2](#)
- [41] Xinyang Yi, Ji Yang, Lichan Hong, Derek Zhiyuan Cheng, Lukasz Heldt, Aditee Kumthekar, Zhe Zhao, Li Wei, and Ed Chi. Sampling-Bias-Corrected Neural Modeling for Large Corpus Item Recommendations. In *Proceedings of the 13th ACM Conference on Recommender Systems*, New York, NY, USA, 2019. Association for Computing Machinery. [3, 8](#)
- [42] Georgios Zoumpourlis, Alexandros Doumanoglou, Nicholas Vretos, and Petros Daras. Non-linear convolution filters for cnn-based learning. *CoRR*, abs/1708.07038, 2017. [2](#)